Reaction Mechanism of Compound I Formation in Heme Peroxidases: A Density Functional Theory Study

Maria Wirstam, Margareta R. A. Blomberg, and Per E. M. Siegbahn*

Contribution from the Department of Physics, Stockholm University, Box 6730, S-113 85 Stockholm, Sweden

Received June 14, 1999. Revised Manuscript Received August 23, 1999

Abstract: The mechanisms for O−O bond breaking in heme peroxidases have been studied using hybrid density functional theory (DFT-B3LYP). The chemical model used to study the reaction includes both the distal and the proximal imidazole. The reaction starts with the transfer of a proton from the peroxide to the distal imidazole, which is found to occur without any barrier using the present model. In the next step, the proton is donated back from the histidine to the other oxygen of the peroxide, with a simultaneous breaking of the O−O bond of the peroxide. This part of the reaction is found to be quite complicated with involvement of three different potential surfaces. The transition state is found to be determined by a crossing between two of these surfaces. The calculated barrier, as determined by the crossing point using a frozen reaction coordinate, is 10.4 kcal/mol, which is in reasonable agreement with the experimental barrier height of 6.5 kcal/mol. After passage of the barrier, compound I is formed. This complex was studied in detail using a full representation of the proximal His-Asp-Trp triad present in cytosolic ascorbate peroxidase and cytochrome *c* peroxidase. In this model the radical is shared equally between the porphyrin and the tryptophan, which is found to be cationic in agreement with most experiments. The results are compared to experiments and other calculations.

I. Introduction

Heme-containing peroxidases are enzymes that can oxidize a variety of substrates by reacting with hydrogen peroxide. For most peroxidases the typical substrates are small aromatic molecules. An exception is cytochrome *c* peroxidase (CCP) found in the mitochondria electron transport chain, which has a protein, cytochrome *c*, as its redox partner. The first structures of a peroxidase were determined for yeast cytochrome *c* peroxidase.[1−3] Later, structures for several peroxidases have been obtained including lignin peroxidase (LIP),[4] pea cytosolic ascorbate peroxidase (APX),[5] peanut peroxidase (PNP),[6] and horseradish peroxidase (HRP).[7] The region around the active site of CCP is illustrated in Figure 1. The histidine and aspartic acid in the proximal heme pocket are present at this position in all structurally characterized peroxidases, whereas the proximal tryptophan is only present in CCP and APX. In most peroxidases this position is occupied by phenylalanine. The histidine, tryptophan, and arginine in the distal pocket shown in Figure 1 are present in all known heme peroxidases.

In Figure 2 the well-established catalytic cycle of heme peroxidases is illustrated. The first step of the reaction leads

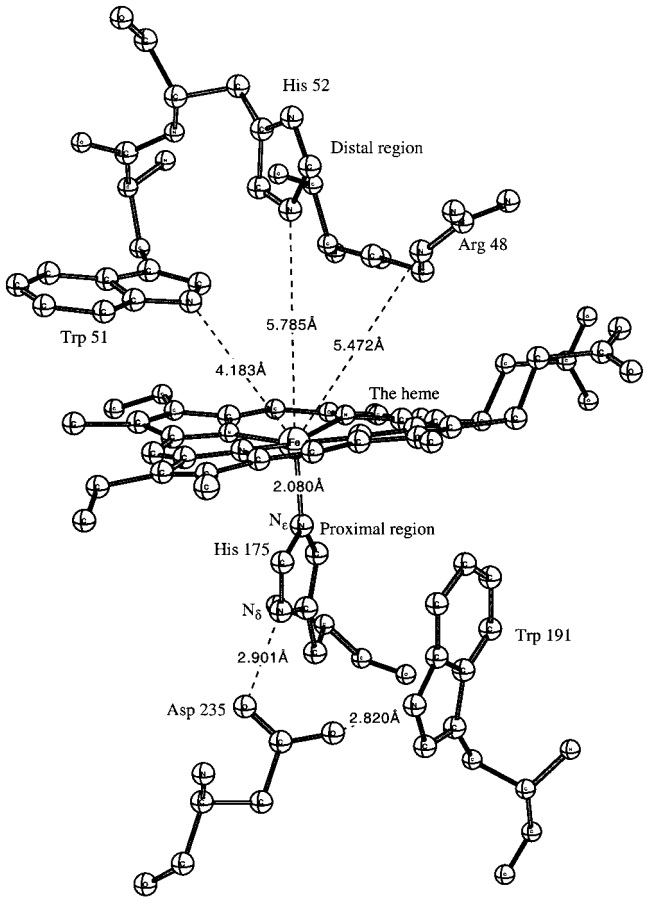

Figure 1. Active site of yeast cytochrome *c* peroxidase based on the X-ray crystal structure.[3]

(1) Poulos, T. L.; Freer, B. T.; Alden, R. A.; Xuong, N.-H.; Edwards, S. L.; Hamlin, R. C.; Kraut, J. *J. Biol. Chem.* **1978**, *253*, 3730−3735.
(2) Poulos, T. L.; Freer, B. T.; Alden, R. A.; Edwards, S. L.; Skoglund, U.; Takio, K.; Eriksson, B.; Xuong, N.; Yonetani, Y.; Kraut, J. *J. Biol. Chem.* **1980**, *255*, 575−580.
(3) Finzel, B. C.; Poulos, T. L.; Kraut, J. *J. Biol. Chem.* **1984**, *269*, 32759−32767.
(4) Poulos, T. L.; Edwards, S. L.; Wariishi, H.; Gold, M. H. *J. Biol. Chem.* **1993**, *268*, 4429−4440.
(5) Patterson, W. R.; Poulos, T. L. *Biochemistry* **1995**, *34*, 4342−4345.
(6) Schuller, D. J.; Ban, N.; van Huystee, R. B.; McPherson, A.; Poulos, T. L. *Structure* **1996**, *4*, 311−321.
(7) Gajhede, M.; Schuller, D. J.; Henriksen, A.; Smith, A. T.; Poulos, T. L. *Nature Struct. Biol.* **1997**, *4*, 1032−1038.

10.1021/ja991997c CCC: $18.00
Published on Web 11/03/1999

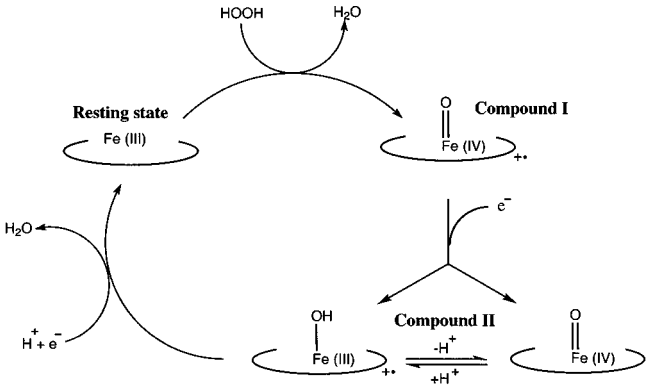

Figure 2. Fundamental steps of the catalytic cycle of heme peroxidases.

from the resting ferric state to an oxyferryl state with a simultaneous formation of a radical. For the majority of the peroxidases, the radical is located on the porphyrin of the heme, giving the intermediate known as compound I. However, in CCP the radical center has been determined to be Trp 191, which is connected to the heme via the hydrogen-bonded His-Asp-Trp triad as illustrated in Figure 1. The oxyferryl intermediate in CCP is also often referred to as compound ES. The absence of a radical on an amino acid residue in PNP and HRP can be explained by the fact that the position corresponding to the Trp 191 residue in CCP in those enzymes is occupied by phenylalanine, which is harder to oxidize. The reason why it is not observed in APX, which actually has a tryptophan residue (Trp 179) at this position, has been suggested to be the presence of a potassium cation located about 8 Å from the proximal tryptophan in APX but not in CCP.[5] This cation has been suggested to affect the electrostatic environment around the tryptophan residue, leading to destabilization of the tryptophan radical in APX relative to CCP. Other residues have also been suggested to contribute to the destabilization of the radical.[8] The role of the alkali cation present in APX has also been investigated by studies of mutated CCP, which like APX binds a cation. For the mutant, the electron-transfer rate from cytochrome *c* to CCP was less than 1% of the rate measured for the wild-type enzyme. On the other hand, the activity toward typical APX substrates was shown to increase.[9] CCP is designed to oxidize ferrous cytochrome *c* and therefore requires an electron-transfer (ET) pathway out to the protein surface. Trp 191 has been suggested to be involved in the ET via a pathway leading from the heme of cytochrome *c* to the backbone of Trp 191.[10] However, mutation experiments have shown that Trp 191 is not essential for ET,[11,12] which indicates that there are alternative pathways.

The large similarities between the active sites of different heme peroxidases indicate a common reaction mechanism for O−O bond cleavage in these enzymes. The roles of the different amino acids around the heme have been studied by use of site-directed mutagenesis. For both CCP[13] and HRP[14] it has been shown that replacement of His 52 by a leucine residue decreases the rate for compound I formation by 5 orders of magnitude. The effect of replacing the distal arginine is less significant, giving only a 2-fold decrease of the reaction rate. These results indicate that the distal His 52 is the most essential amino acid for catalytic activity. On the basis of the X-ray crystal structure of CCP it has been proposed that His 52 functions as an acid−base catalyst as indicated in Figure 3.[15] In this mechanism His 52 first abstracts a proton from one of the oxygens of HOOH as a base and in the next step protonates the other oxygen as an acid, which in turn leads to formation of water and compound I. The roles of the distal tryptophan and arginine residues are somewhat uncertain although it has been suggested that their function could be to stabilize the transition state for formation of compound I.

In the present study the electronic structure of compound I and the mechanism of compound I formation are investigated by use of density functional theory (DFT). Several theoretical studies contributing to the understanding of peroxidases have been performed earlier.[8,16−19] However, this is the first quantum chemical study of the mechanism aimed at locating a transition state for the O−O bond splitting and also the first one where a reasonably realistic model of the region around the heme has been used. This means a model including both the distal and the proximal imidazole. The transition state was located by performing geometry optimizations where the critical O−O and O−H bond lengths were frozen and varied independently. The transition state was found to be determined by a crossing between two different potential energy surfaces. Furthermore, full DFT geometry optimizations have for the first time been performed on models including the entire His-Asp-Trp triad of CCP and APX to determine the position of the protons in the hydrogen bonds in compound I and also to analyze the charge and spin distribution in the cluster.

II. Computational Details

The calculations were performed in two steps. First, an optimization of the geometry was performed using the B3LYP method.[20,21] Double-ζ basis sets were used in this step. In the second step the energy was evaluated for the optimized geometry using large basis sets including diffuse functions and with a single set of polarization functions on each atom. The final energy evaluation was also performed at the B3LYP level. All the calculations were carried out using the GAUSSIAN programs.[22,23]

In the B3LYP geometry optimizations, the LANL2DZ set of the GAUSSIAN program was used. For iron this means that a nonrelativistic effective core potential (ECP) according to Hay and Wadt[24] was used. The valence basis set used in connection with this ECP is

(8) Jensen, G. M.; Bunte, S. W.; Warshel, A.; Goodin, D. B. *J. Phys. Chem. B* **1998**, *102*, 8221−8228.
(9) Bonagura, C. A.; Sundaramoorthy, M.; Pappa, H. S.; Patterson, W. R.; Poulos, T. L. *Biochemistry* **1996**, *35*, 6107−6115.
(10) Pelletier, H.; Kraut, J. *Science* **1992**, *258*, 1748−1755.
(11) Choudhury, K.; Sundaramoorthy, M.; Mauro, J. M.; Poulos, T. L. *J. Biol. Chem.* **1992**, *267*, 25656−25659.
(12) Choudhury, K.; Sundaramoorthy, M.; Hickman, A.; Yonetani, T.; Woehl, E.; Dunn, M. F.; Poulos, T. L. *J. Biol. Chem.* **1994**, *269*, 20239−20249.
(13) Erman, J. E.; Vitello, L. B. *J. Am. Chem. Soc.* **1992**, *114*, 6592−6593.
(14) Rodriguez-Lopez, J. N.; Smith, A. T.; Thorneley, R. N. F. *J. Biol. Inorg. Chem.* **1996**, *1*, 136−142.
(15) Poulos, T. L.; Kraut, J. *J. Biol. Chem.* **1980**, *255*, 8199−8205.
(16) Náray-Szabó, G. *J. Biol. Inorg. Chem.* **1997**, *135*, 135−138.
(17) Harris, D. L.; Loew, G. H. *J. Am. Chem. Soc.* **1996**, *118*, 10588−10594.
(18) Harris, D. L.; Loew, G. H. *J. Am. Chem. Soc.* **1996**, *118*, 10584−10587.
(19) Kuramochi, H.; Noodleman, L.; Case, D. A. *J. Am. Chem. Soc.* **1997**, *119*, 11442−11451.
(20) Becke, A. D. *Phys. Rev.* **1988**, *A38*, 3098. Becke, A. D. *J. Chem. Phys.* **1993**, *98*, 1372. Becke, A. D. *J. Chem. Phys.* **1993**, *98*, 5648.
(21) Stevens, P. J.; Devlin, F. J.; Chablowski, C. F.; Frisch, M. J. *J. Phys. Chem.* **1994**, *98*, 11623.
(22) Frisch, M. J.; Trucks, G. W.; Schlegel, H. B.; Gill, P. M. W.; Johnson, B. G.; Robb, M. A.; Cheeseman, J. R.; Keith, T.; Petersson, G. A.; Montgomery, J. A.; Raghavachari, K.; Al-Laham, M. A.; Zakrzewski, V. G.; Ortiz, J. V.; Foresman, J. B.; Cioslowski, J.; Stefanov, B. B.; Nanayakkara, A.; Challacombe, M.; Peng, C. Y.; Ayala, P. Y.; Chen, W.; Wong, M. W.; Andres, J. L.; Replogle, E. S.; Gomperts, R.; Martin, R. L.; Fox, D. J.; Binkley, J. S.; Defrees, D. J.; Baker, J.; Stewart, J. P.; Head-Gordon, M.; Gonzalez, C.; Pople, J. A. *Gaussian 94*, Revision B.2; Gaussian Inc.: Pittsburgh, PA, 1995.

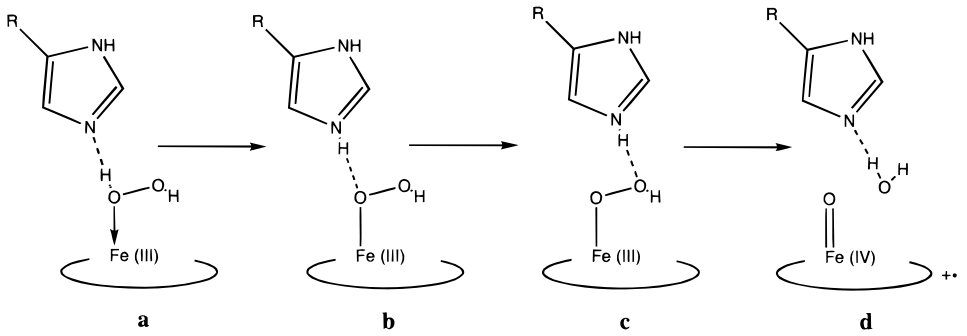

Figure 3. The proposed mechanism of compound I formation in heme peroxidases. First, hydrogen peroxide enters the active site (a). In the next step the distal histidine abstracts a proton from peroxide. Simultaneously, a covalent bond is formed between iron and one of the oxygens (b). The proton is then donated back to form water and compound I (c,d).

essentially of double-ζ quality. The rest of the atoms are described by standard double-ζ basis sets. In the B3LYP energy calculations the diffuse and polarization functions from the 6-311+G(1d,1p) basis sets in the GAUSSIAN program were added to the LANL2DZ basis sets. This basis set has a single set of polarization functions on all atoms including f-sets on iron, and also diffuse functions.

Usually, solvent effects on the relative energies due to the surrounding protein are quite small for reactions where the charge state of the cluster is constant. In contrast, these effects become important when energies of differently charged clusters are compared. The relative energies reported below are therefore gas-phase values except for the ionization energies and hydrogen bond strengths to charged clusters where solvent effects have been added to the final energies.

The approach used for treating the solvent effects is the self-consistent isodensity polarized continuum model (SCI-PCM) as implemented in the GAUSSIAN-94 program.[25] The default isodensity value of 0.0004 e/B^3 was used, which has been found to yield volumes very close to the observed molar volumes. The dielectric constant of the protein is the main empirical parameter of the model and it was chosen to be equal to 4 in line with previous suggestions for proteins.

In the text below, different nomenclature is used for discussing spin states depending on the situation. For example a doublet spin state means that the multiplicity ($2S + 1$) is equal to 2, giving the spin (S) equal to 1/2. When the spin population is discussed, it is expressed in numbers of unpaired electrons. This means that if a certain group has one unpaired electron, the spin population on this group is equal to 1.

III. Results and Discussion

The present section on the results of the model calculations is divided into two subsections. In the first subsection, the chemical features of compound I are discussed. In particular, the spin and the charge states of the tryptophan residue are discussed. For these investigations a model is used where the entire proximal His-Asp-Trp triad is represented. In the second subsection, the O−O bond-breaking reaction is discussed in detail. For this part of the present study, the distal histidine is included in the model while the proximal triad is modeled by a single imidazole group. The O−O bond-breaking reaction is shown to occur in steps where the final step is quite complicated with a barrier determined by a crossing between two different potential energy surfaces.

(a) Chemical Features of Compound I. The first question investigated for compound I of peroxidases (see Figure 2) is the spin of the ground state. For this investigation a neutral imidazole ligand is kept in the proximal heme pocket and the porphyrin is replaced by two (NH)(CH)$_3$(NH) groups which form two rings that bind to iron. The net charge of this model is +1. The same model is used to study the mechanism for formation of compound I, discussed in subsection IIIb below. Using this model a quartet ground state was obtained. Approximately two of the unpaired electrons reside in the Fe=O group (1.19 on Fe and 1.08 on O) and the remaining one (0.79) is located on the porphyrin analogue. In an orbital description, there are two unpaired electrons in the degenerate Fe=O π^* antibonding orbital that are triplet coupled, coupled to an unpaired electron on porphyrin.[26]

A critical question when this rather small heme model is used is whether the ionization potential of the heme is correctly reproduced. This is important since in the proposed O−O splitting mechanism investigated below the heme group is expected to become cationic. A comparison of computed ionization potentials of the oxyferryl state (O−Heme[Fe(IV)]), using the small heme model described above and for a larger heme model including the porphyrin and also the propionates of the actual heme, gave a difference of only 2 kcal/mol. This shows that the smaller heme model is quite adequate, at least in this respect. For this larger heme model the spin distribution is only slightly different from the one obtained using the small Fe−2(NH)(CH)$_3$(NH) model, giving spin populations of 1.15 on Fe, 0.89 on O, and 0.96 on porphyrin. Furthermore, Kuramochi et al.[19] have made single-point nonlocal DFT calculations using a triple-ζ basis set on a model where the porphyrin was used in the heme model. In that study, also a quite similar spin distribution was obtained, with values on Fe, O, and porphyrin of 1.24, 0.99, and 0.78, respectively. The similarities between the spin distributions obtained for the different models give additional indications that the simplified porphyrin model should give reasonable results. In addition to the quartet state with approximately $S = 1$ on the Fe−O moiety ferromagnetically coupled to the $S = 1/2$ on porphyrin, there should also be an energetically close-lying doublet state where the spin on Fe−O is antiferromagnetically coupled to the spin on porphyrin. Unfortunately, convergence to this doublet state could not be obtained. However, in the study performed by Kuramochi et al. the $^4A_{2u}$ and the $^2A_{2u}$ states were found to be

(23) Frisch, M. J.; Trucks, G. W.; Schlegel, H. B.; Scuseria, G. E.; Robb, M. A.; Cheeseman, J. R.; Zakrzewski, V. G.; Montgomery, J. A., Jr.; Stratmann, R. E.; Burant, C. J.; Dapprich, S.; Millam, J. M.; Daniels, A. D.; Kudin, K. N.; Strain, M. C.; Farkas, O.; Tomasi, J.; Barone, V.; Cossi, M.; Cammi, R.; Mennucci, B.; Pomelli, C.; Adamo, C.; Clifford, S.; Ochterski, J.; Petersson, A. G.; Ayala, Y. P.; Cui, Q.; Morokuma, K.; Malick, K. D.; Rabuck, D. A.; Raghavachari, K.; Foresman, B. J.; Cioslowski, J.; Ortiz, V. J.; Stefanov, B. B.; Liu, G.; Liashenko, A.; Piskorz, P.; Komaromi, I.; Gomperts, R.; Martin, L. R.; Fox, J. D.; Keith, T.; Al-Laham, A. M.; Peng, Y. C.; Nanayakkara, A.; Gonzalez, C.; Challacombe, M.; Gill, P. M. W.; Johnson, B.; Chen, W.; Wong, M. W.; Andres, J. L.; Gonzalez, C.; Head-Gordon, M.; Replogle, E. S.; Pople, J. A. *Gaussian 98*, Revision A.3; Gaussian, Inc.: Pittsburgh, PA, 1998.

(24) Hay, P. J.; Wadt, W. R. *J. Chem. Phys.* **1985**, *82*, 299.

(25) Wiberg, K. B.; Keith, T. A.; Frisch, M. J.; Murcko, M. *J. Phys. Chem.* **1995**, *99*, 9072.

(26) Filatov, M.; Harris, N.; Shaik, S. *J. Chem. Soc., Perkin Trans.* **1999**, *2*, 399−410.

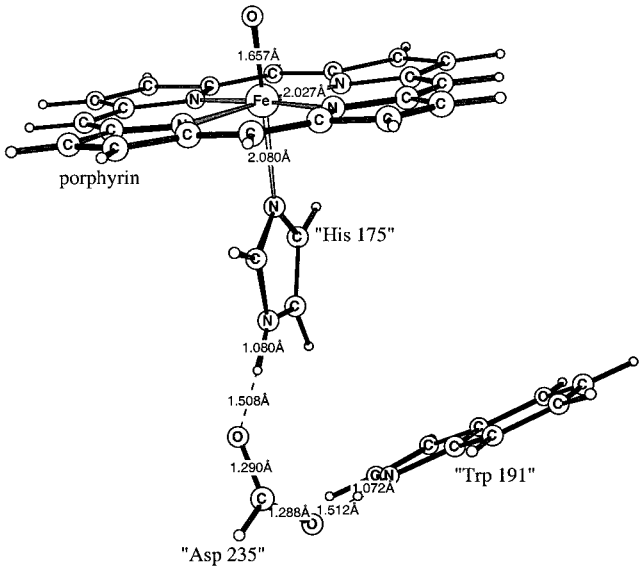

Figure 4. Fully optimized model structure of compound I of APX and CCP. The amino acid numbering is for CCP. The spin and charge distribution of different parts of the complex are given in Table 1.

essentially degenerate. Also, the spin distribution obtained for the $^4A_{2u}$ state was found to be close to that for the $^2A_{2u}$ state except that the spin on porphyrin in the doublet state is in the opposite direction. In the following discussion, only the quartet of these near-degenerate states was therefore considered. The excitation energy from the quartet to the sextet state was in the present study found to be 22.2 kcal/mol. This state has a spin population of 2.92 on Fe, 0.89 on O, and 1.19 on the porphyrin model.

As discussed in the introduction, for certain peroxidases the radical in compound I is located on an amino acid residue rather than on the heme ring. Therefore the second question investigated here concerns the character of the tryptophan radical formed in compound I of CCP. Although some results could be interpreted in terms of a formation of a neutral oxidized indole in CCP,[27,28] most studies indicate that it should be cationic.[29] The model of the active sites of CCP and APX used to study this question is based on the crystal structures,[1,5] and includes a full unsubstituted iron porphyrin and the functional groups of all three proximal amino acids shown in Figure 1. His 175 was thus modeled by an imidazole, Asp 235 by a formate, and Trp 191 by an indole (numbering referring to CCP), giving a total number of 67 atoms in the quantum chemical model. Using this model, full geometry optimizations were performed starting with different locations of the protons between His 175 and Asp 235 on one hand and between Asp 235 and Trp 191 on the other hand. The lowest energy was obtained for the structure shown in Figure 4. Since the distal amino acids should have only a minor influence on the charge state of the tryptophan these were not included in the model. The total spin (S) used for the calculation was 3/2 (^{4}A), in line with the ground state obtained (see above), and the complex was considered to be neutral.

It should be noted that the accuracy of computed bond distances and angles is usually higher than what is obtained by X-ray crystallography.[30,31] However, some geometrical features may be incorrectly reproduced due to the choice of a limited model. For example, during the optimization the tryptophan moves from its initial position observed in the X-ray structures due to the lack of a representation of steric effects from parts of the protein not included in the model. However, it is unlikely that this deficiency of the model should severely affect the electronic structure and total energy of the complex.

Table 1. Mulliken Spin (S) and Charge (Q) Distributions for the Modeled Compound I/ES Complex Shown in Figure 4[a]

group	Q	S
Fe	0.16	0.95
O	−0.19	1.10
porphyrin	+0.21	0.48
"His 175"	+0.22	
"Asp 235"	−0.68	
"Trp 191"	+0.28	0.47
total	0	3

[a] The amino acid numbering is for CCP. Values less than 0.02 are omitted.

By only considering the bond distances of the structure in Figure 4 it is found that the tryptophan clearly is protonated, with a proton distance of 1.07 Å to the indole nitrogen and 1.51 Å to the carboxylate group. It is furthermore clear that the proton between the imidazole and the carboxylate is much closer to the imidazole. In Table 1, the Mulliken charge and spin distributions for the cluster are shown. The charge distribution shows that the indole, imidazole, and porphyrin are all positively charged with values between +0.2 and +0.3. The charge on carboxylate is, as expected, negative and the value obtained is −0.68.

It could be argued that the determination of the position of a proton could be quite uncertain based on the present gas-phase-type calculations, and that ideally the protein should be included in a QM-MM procedure. However, in the present case where the gas-phase model favors the charge-separated system, $Asp^- - TrpH^+$, the introduction of the protein is only expected to make this state even more favored compared to the case without charge separation. Instead, in this case it is more important to use a method, like B3LYP with full geometry optimization, so that all the relevant resonances for the indol cation−radical are correctly described. These resonances are very important for the proton affinity, as can be seen on a comparison between the gas-phase proton affinities of the indol and pyrrol radicals, which is as much as 8.7 kcal/mol larger for the indol radical. It is furthermore of interest to note that the gas-phase phenol radical has a proton affinity that is 23.6 kcal/mol smaller than that of indol, which is a good explanation for the fact that tyrosyl radicals are neutral while tryptophan radicals are usually protonated in enzymes.

The Mulliken population analysis further gives a spin population on the Fe═O moiety of 2.05. Most of the remaining spin population of 0.95 is, interestingly, shared equally between tryptophan and the porphyrin in spite of the long distance between the porphyrin and the indole obtained in the optimized structure. This indicates that the difference in ionization potential between tryptophan and porphyrin for the oxyferryl form of APX and CCP must be small. This is in line with the observations that the location of the radical varies with the different environments in APX and CCP.[9,16,28] The largest part (41%) of the spin population on tryptophan is located on the carbon that leads out to the backbone. This agrees well with

(27) Krauss, M.; Garmer, D. R. *J. Phys. Chem.* **1993**, *97*, 831−836.
(28) Menyhárd, D. K.; Náray-Szabó, G. *J. Phys. Chem. B* **1999**, *103*, 227−233.
(29) Stubbe, J.; van der Donk, W. A. *Chem. Rev.* **1998**, *98*, 705−762.
(30) Pierloot, K.; De Kerpel, J. O. A.; Ryde, U.; Olsson, M. H. M.; Roos, B. O. *J. Am. Chem. Soc.* **1998**, *120*, 13156−13166.
(31) Bauschlicher, C. W., Jr.; Ricca, A.; Partridge, H.; Langhoff, S. R. In *Recent Advances in Density Functional Methods, Part II*; Chong, D. P., Ed.; World Scientific Publishing Company: Singapore, 1997; p 165.

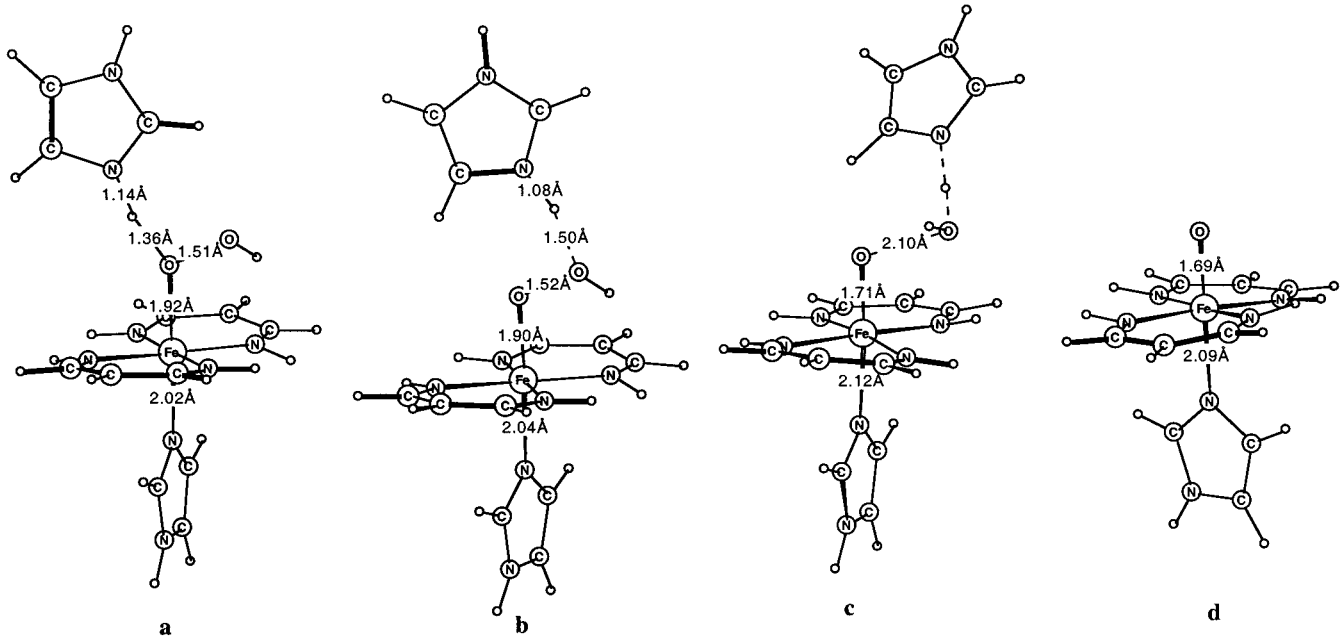

Figure 5. Optimized intermediates of modeled heme peroxidases. The relative energies are shown in Figure 6 and Table 3.

electron nuclear double resonance (ENDOR) experiments performed on CCP[32] from which exactly the same percentage of the spin on Trp 191 was found to be located on that carbon. However, it should be pointed out that the total spin density on Trp 191 obtained in these experiments is equal to 1, in contrast to our results on the model compound with a total spin population on tryptophan of only 0.47. A radical formed on this carbon fits nicely into the picture of an ET pathway in CCP that follows the backbone chain leading from Trp 191 to the heme of cytochrome *c*.[11]

During the last years several other theoretical studies have contributed to the understanding of compound I. The first DFT calculations of compound I models were performed by Kuramochi et al. for a model that includes the full unsubstituted iron porphyrin ring modeling the heme and the proximal imidazole.[19] In that study the molecular orbitals for the ground state of compound I of heme peroxidases were analyzed in detail using the geometry obtained from the X-ray structure. Furthermore, the energetics of the redox process between compound I and compound II was also discussed.[19] The redox potential for compound I was computed to be 1.61 V for the gas phase and 0.56 V for the aqueous solution, which can be compared with the experimentally determined redox potential for compound I of HRP of 0.95 V. In a study by Menyhárd et al.[28] electrostatic potential and single-point Hartree−Fock calculations using minimal basis sets were performed for different protonation states of the His-Asp-Trp triad and compared to experimental ENDOR results. In contrast to our results it was found that the radical could appear on tryptophan only if this residue is deprotonated by the neighboring aspartate. The conclusion was that the difference between CCP and APX could be explained by different locations of the protons in the distal heme region, which is a consequence of different protein environments of these enzymes. However, the present results, including fully optimized structures at a high level of theory, indicate that the radical appears on a protonated tryptophan in CCP, which furthermore is in agreement with most experimental studies.[29] Finally, the protein environment of CCP and APX has been studied theoretically using the protein dipoles Langevin dipoles (PDLD) model combined with molecular dynamics.[8] From these calculations it was concluded that the protein environment of CCP stabilizes the tryptophan radical relative to that of APX. The alkali cation and its ligand Asp 187 together destabilize the tryptophan cation radical of APX by 7.1 kcal/mol. However, it was also found that there are several other small contributions to the destabilization of the tryptophan radical of APX relative to that of CCP.

(b) Mechanism of Compound I Formation. The main part of the present study concerns the reaction mechanism for the O−O bond cleavage shown in Figure 3, which was proposed on the basis of the X-ray structure.[15] While the entire heme-His-Asp-Trp part could be accurately modeled when the chemical features of compound I were studied, a smaller model of the active site had to be used when the more complicated study of the reaction mechanism was performed. For the heme, the smaller model discussed in subsection IIIa and shown in Figure 5 was used. To further limit the computational cost, only the histidine residue was kept in the proximal pocket. At first sight it may seem that this model could not represent the O−O bond cleavage process in heme peroxidases like CCP where the proximal tryptophan, which is not included in the model, eventually becomes oxidized. However, a strong indication that the proximal tryptophan does not need to become oxidized in the actual O−O bond cleavage process is that the reaction rate for compound I formation in HRP[14] was found to be very similar to the rate obtained for CCP[13] in spite of the fact that HRP has a phenylalanine at the position for Trp 191 of CCP. The results reported in subsection IIIa indicating similar reaction energies for formation of a radical on porphyrin and on Trp 191 are also in line with these findings. Therefore, the investigation of the mechanism should be representative for all heme peroxidases even though the proximal tryptophan is not included in this model. The distal histidine, which was not included in the model used in the previous subsection, has to be included in the model when the reaction mechanism of Figure 3 is examined, since it is known to be essential for catalysis[13,14] and directly involved in the proposed reaction mechanism shown in Figure 3. Using such a complex, there is still a choice of charge state. The

(32) Huyett, J. E.; Doan, P. E.; Gurbiel, R.; Houseman, A. L. P; Sivaraja, M.; Goodin, D. B.; Hoffman, B. M. *J. Am. Chem. Soc.* **1995**, *117*, 9033−9041.

histidine in the proximal pocket could be considered to be deprotonated and thus modeled by an imidazolate. This approach would result in a neutral model complex. Alternatively, a neutral imidazole could be used to model the proximal pocket, giving a net charge of +1 for the model complex. The optimized structure of the entire O═Heme-His-Asp-Trp part, discussed in the previous subsection, indicates that in compound I, the proton is clearly closer to the histidine than to the aspartate. Also for the resting ferric state similar calculations, but using a smaller heme-model, show that the proton between the histidine and the aspartate is somewhat closer to histidine, with a distance of 1.15 Å to the imidazole nitrogen and 1.36 Å to the aspartate oxygen. These results indicate that the His-Asp-chain may perhaps be best modeled by a neutral imidazole, and thus with a charge of +1 for the total complex.

Using a positively charged model as described above, attempts were first made to optimize a reactant where hydrogen peroxide coordinates to the iron of the heme and forms a hydrogen bond to the distal histidine as shown in Figure 3a. However, no stable structure for such a complex was found. Instead, the proton moves from the peroxide to the imidazole without passing a barrier during geometry optimization. Studies of the proton transfer energy barriers in $H_5O_2^+$ [33] indicate that the B3LYP functional sometimes tends to underestimate barriers for proton transfers by 0−2.5 kcal/mol compared to results obtained using CCSD(T). This means that a small barrier for proton transfer cannot be ruled out. However, a possible small barrier for the proton transfer should have no effect on the rate for the overall reaction as long as it is lower than the barrier for breaking the O−O bond, see further below. The optimized structure for the product of the proton transfer is shown in Figure 5a. The lowest energy for this complex is obtained for a doublet spin state. Mulliken population analysis for the converged structure shows that all spin is located on iron. As shown by the distances given in Figure 5a, the proton is not entirely located on imidazole, but there is also a rather short distance to the OOH^- group. The charge on iron in this state is +0.62, while the charge on the proximal imidazole is +0.34 and that of the distal OOH^-−H^+His group is +0.38. The charge obtained for the porphyrin model is −0.34. These values can be compared to results obtained for a model of the resting ferric state using a complex that includes the heme and the proximal imidazole. For this state the charge on iron is +0.90 and the charges on imidazole and porphyrin model are +0.27 and −0.17, respectively. Thus, when hydrogen peroxide reacts with the active site, positive charge is transferred mainly from iron (0.28) and from the porphyrin model (0.17) to the distal heme pocket. Since the charge transfers may be sensitive to the total charge state of the model chosen, these calculations were also performed using an overall neutral model in which an imidazolate was used for His 175. For the neutral model positive charges of 0.34 and 0.10 are transferred from iron and the porphyrin analogue, compared to 0.28 and 0.17 for the positively charged model, indicating that these models behave quite similarly.

In the next step of the proposed peroxidase reaction, the hydrogen bond between histidine and the peroxide should switch from the proximal to the distal oxygen as shown in the step **b**−**c** of Figure 3. The details of this step have not been investigated in the present study, which mainly has focused on the O−O bond-breaking mechanism. The shift of the hydrogen bond could, for example, be assisted by an arginine residue in this region or by water molecules that have also been observed in structural studies of this region. Using a naked Mg^{2+} ion, Woon and Loew showed that the barrier for transforming Mg^{2+}−HOOH into Mg^{2+}−OOH_2 was significantly lowered in the presence of a water molecule that acts as base.[34] Using the present model the energy goes up by 5.3 kcal/mol in this step (**b**−**c** in Figure 3), giving the structure shown in Figure 5b. We consider this energy increase as a probable artifact of the limited model, and the energies will hereafter be given relative to the energy for the structure in Figure 5b. Also for this intermediate the ground state is a doublet ($S = 1/2$), which agrees with results obtained from other theoretical studies.[17] The excitation energies to the quartet and sextet states were found to be 11.0 and 13.9 kcal/mol, respectively. During this reaction step the charge distribution of the cluster changes somewhat. The positive charge on iron decreases by 0.07 to a value of +0.55. At the same time the positive charge of the OOH^-−H^+imidazole group increases by 0.10 to a value of +0.48. The charges on the proximal imidazole and porphyrin model are on the other hand almost unaltered. In summary, the charge and spin populations change only slightly in the step **b**−**c** of Figure 3.

In the final step of the reaction the proton should be donated back from the histidine to the distal oxygen of OOH^- followed by cleavage of the O−O bond and formation of the product of the reaction shown as **d** of Figure 3. This is by far the most complicated part of the reaction and a considerable number of model studies were required for the investigation of this step. In the present model the barrier is determined by a spin-crossing between a quartet and a doublet surface. In reality, the reaction path in this region could instead involve the antiferromagnetically coupled doublet state rather than the quartet state. As mentioned above, these states are very nearly degenerate and electronically very similar. Involvement of the antiferromagnetic doublet would formally avoid a specific spin-crossing, but due to the large change of electronic structure character there would still be a sharply avoided crossing at a very similar energy, and the present model should therefore still yield a qualitatively correct barrier.

The reaction coordinate between **c** and **d** of Figure 3 could reasonably well be described by two structural parameters: the O−O distance of the OOH^- group and the distance between the distal oxygen of OOH^- and the proton on histidine. These two bond distances were varied independently for both quartet and doublet states to set up a grid of energy points. In each point, geometry optimizations were performed where the O−O and the O−H distances were kept frozen and all other structural parameters optimized. By performing this two-dimensional search of the potential surface, it was found that the critical parameter for this reaction is the O−O bond distance, while the proton could be moved from histidine to OOH^- almost freely without any barrier for different O−O distances along the reaction path.

Figure 6 shows the energy changes for different O−O bond distances along the reaction. The relative energies are further given in Table 3. Starting from the doublet Heme[Fe(III)]−OOH−H^+His complex (Figure 5b) the energy first increases with the O−O bond distance on the doublet surface. For O−O distances less than 1.80 Å, essentially all spin is located on iron, as in the reactant. In this region, the distance between iron and the proximal oxygen decreases from 1.92 to 1.85 Å. For O−O distances larger than 1.80 Å there is a sudden change of behavior, and the energy increases much slower with the oxygen distance as shown in Figure 6. Simultaneously, negative spins

(33) Sadhukhan, S.; Muños, D.; Adamo, C.; Scuseria, G. E. *Chem. Phys. Lett.* **1999**, *306*, 83−87.

(34) Woon, D. E.; Loew, G. H. *J. Phys. Chem. A* **1998**, *102*, 10380−10384.

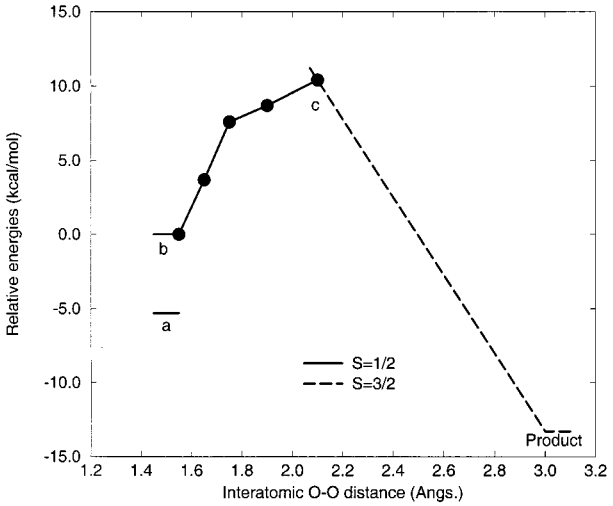

Figure 6. The potential energy surface for modeled compound I formation in heme peroxidases. The labels refer to Table 3 and to the structures shown in Figure 5.

Table 2. Mulliken Spin (*S*) and Charge (*Q*) Distributions in the Modeled Reactant [HisH-HOO-Hem-His]$^+$ (b of Figure 5) and Product [His-HOH-O-Hem-His]$^+$ of the HOOH Activation in Heme Peroxidases[a]

group	*Q*(reactant)	*Q*(product)	*S*(reactant)	*S*(product)
Fe	+0.55	+0.45	0.94	1.19
O		−0.21		1.08
OOH	−0.37			
"porphyrin"	−0.36	+0.32		0.79
"His 52"	+0.85	+0.11		
"His 175"	+0.33	+0.22		
total	+1.00	+1.00	1.00	3.00

[a] The amino acid numbering is for CCP. Spin populations less than 0.02 are omitted.

Table 3. Relative Energies (ΔE) on the Potential Energy Surface for HOOH Activation by Heme Peroxidases[a]

compound	ΔE (kcal/mol)
[HisH-OOH-Hem-His]$^+$ (a)	−5.3
[HisH-HOO-Hem-His]$^+$ (b)	0.0
transition state (c)	10.4
[His-HOH-O-Hem-His]$^+$	−13.3

[a] The letters in parentheses refer to the corresponding letters in Figure 5.

appear on the oxygens. These are strong indications that an avoided potential surface crossing has occurred and that the reaction has passed over to another doublet potential surface of a different character. For an O−O distance of 1.90 Å, spin populations of 1.09 on iron and −0.23 on the distal oxygen were obtained. The spin on the porphyrin model is 0.07 and the spin on the proximal oxygen 0.09. At a distance of 2.10 Å the spin on iron increases further to 1.59. For this geometry, the spin population on the distal oxygen is −0.30 and on the proximal oxygen −0.35. The spin on the porphyrin model is still small for the doublet state at this O−O distance, with a value of only 0.08. At this O−O distance of 2.10 Å, the optimized quartet state has the same energy and a spin-crossing occurs as shown in Figure 6. In the actual peroxidase system this point could also correspond to a crossing between a doublet surface which has one unpaired electron located on iron and the oxygens and another doublet surface where two unpaired electrons on the Fe−OOH part is antiferromagnetically coupled to one unpaired electron on the porphyrin analogue. The energy for the quartet state was also calculated in the geometry optimized for the doublet at the O−O distance of 2.10 Å, and was found to be only 4.8 kcal/mol higher than the doublet energy. This is quite important for a possible surface crossover, and shows that the upper limit for reaching a geometrical crossing point is only 4.8 kcal/mol. Based on previous experience, this type of estimate leads to a largely exaggerated energy cost and the actual additional energy required to cross to the other surface should therefore be only 1−2 kcal/mol. In this context it is also quite important that at least one of the surfaces has a very small slope in the crossing region,[35] and as can be seen in Figure 6 the reactant energy on the doublet surface varies only slowly with the critical O−O distance. When the O−O distance changes from 1.75 to 2.10 Å the energy only changes by 2.8 kcal/mol. This allows the reactant to stay in the region of the crossing for sufficiently long times that the crossing can occur. For the quartet state the spin on iron is 1.13. The spin populations on the proximal and distal oxygens are 1.18 and 0.23, respectively, and the spin on the porphyrin model 0.54. This crossing defines the transition state of the reaction. The structure of the doublet state in the crossing point is shown in Figure 5c. The activation energy calculated relative to the reactant shown in Figure 5b is 10.4 kcal/mol. This can be compared to the experimentally known rate for compound I formation in CCP of 3.9×10^7 M^{-1} s^{-1}, which approximately corresponds to a barrier of 6.5 kcal/mol. The agreement between theory and experiment must be considered quite satisfactory considering the complicated nature of the reaction and the limited model used where the porphyrin of the heme is represented by two $(NH)(CH)_3(NH)$ groups. Following the reaction coordinate in the forward direction by relaxing the O−O bond distance and performing a full optimization starting with this geometry leads directly to the formation of compound I and a hydrogen-bonded water as the energy goes down. This compound I−water complex has an energy of −13.3 kcal/mol relative to the structure in Figure 5b. In the final product the spin on the distal oxygen disappears and the spin on the porphyrin model increases to 0.79. It should be noted that it is only when the quartet surface has been reached, that is after the passage of the transition state, that the spin on the porphyrin model starts to build up. In summary, the reaction path along which the O−O bond is broken is quite complicated, passing over three potential surfaces with different character.

The energy of the [Heme$^\bullet$]$^+$[Fe(IV)]═O−HOH−His product is the most uncertain point on the potential energy surface for the reaction, but this is also a less interesting point since the reaction has already been completed. Using the present model, hydrogen bonds are formed between water and the porphyrin model in the converged structure. Although these precise interactions are artifacts due to the chemical model used, hydrogen bonds of similar strength can be formed between water and some other group, for example, the positive arginine residue. Calculations showed that the strength of the hydrogen bonds between water and the porphyrin model, which is cationic at this stage, is 18.9 kcal/mol, which is exactly the same as was obtained for the hydrogen bond between a cationic arginine model and water. Therefore, in spite of the model artifacts, also the energy for the product should be rather reasonable. The problem with the erroneous hydrogen bonds in the [Heme$^\bullet$]$^+$-[Fe(IV)]═O−HOH−His product is the reason why this structure is not shown in Figure 5.

The ground state of compound I is a quartet ($S = 3/2$) or possibly an antiferromagnetically coupled doublet ($S = 1/2$).

(35) Mitchell, S. A. In *Gas-Phase Metal Reactions*; Fontijn, A., Ed.; Elsevier Science Publishers: B.V., 1992; Chapter 12, pp 227−252.

The spin population obtained can also be compared with the case where the entire His-Asp-Trp triad of CCP (or APX) was included in the model. In that case an unpaired electron (0.95) was shared between the porphyrin and the indole as discussed in the previous subsection. During the reaction from Heme-[Fe(III)]−OOH−H^+His (Figure 5b) to [Heme$^{\bullet}$]$^+$[Fe(IV)]═O−HOH−His the net charge of the distal heme pocket changes from +0.48 to −0.10 while the positive charge of the proximal pocket only changes slightly, from +0.22 to +0.33. Also the changes of the charge on iron are small, decreasing from a value of +0.55 in the reactant to +0.45 in the product. The negative charge that appears in the distal heme pocket is donated from the porphyrin analogue, which changes from a charge of −0.36 to +0.32.

For the calculations described above a positively charged model cluster was used. However, preliminary calculations have also been performed on a neutral cluster, modeling His 175 by an imidazolate. The results indicate that the activation energy using such a neutral model for the proposed mechanistic pathway is quite similar to the corresponding energy for the positively charged model. However, the highest point on the potential energy surface for the neutral model seems to occur at a different O−O bond distance and the crossing point between the doublet and the quartet surface in that case may occur after the barrier has been passed.

IV. Conclusions

The present energetic results support the mechanism for compound I formation in heme peroxidases that has been previously proposed based on the X-ray crystal structure for CCP.[15] Upon addition of a hydrogen peroxide molecule to the distal heme pocket, the proton on the proximal oxygen of the peroxide is spontaneously transferred to the distal imidazole resulting in a doublet Heme[Fe(III)]−OOH−H^+His complex. In the following step of the proposed mechanism, the proton on histidine is donated to the distal peroxide oxygen followed by cleavage of the O−O bond. As the O−O bond distance is elongated the energy increases relative to the Heme[Fe(III)]−OOH−H^+His complex and spin appears initially on both oxygens of the O−OH−H group. For an O−O distance of 2.10 Å the complex changes state from a doublet having one unpaired electron to a quartet or an antiferromagnetically coupled doublet having three unpaired electrons, and spin starts to appear also on the modeled porphyrin. The activation energy of the reaction is given by the energy of the crossing between these two states relative to the Heme[Fe(III)]−OOH−H^+His complex (Figure 5b). When the O−O bond is increased in steps while all other degrees of freedom are fully optimized, the crossing occurs at an energy of +10.4 kcal/mol. To reach a true geometric crossing point only a few kilocalories per mole (less than 4.9 kcal/mol and probably only around 1−2 kcal/mol) has to be added to this energy. Following the reaction path for longer O−O distances eventually leads to the final product, which is a model for compound I. In this compound a cationic radical appears on the porphyrin model. If the entire His-Asp-Trp triad of APX and CCP is included in the model the cationic radical is shared between the porphyrin and the protonated indole group. The exothermicity for the O−O splitting reaction was found to be 13.3 kcal/mol relative to the structure shown in Figure 5b. The reasonable values obtained for the activation and reaction energies of the reaction support the reaction mechanism previously proposed[15] although it does not completely rule out alternative pathways.

In the present study we have focused on peroxidases. However, the results obtained should also give valuable insights into the mechanisms for several other O−O splitting heme-enzymes, such as P450, cytochrome *c* oxidase, and catalases. Although the P450 and cytochrome *c* oxidase enzymes catalyze the activation of the oxygen molecule rather than hydrogen peroxide, they are likely to function in a similar way since the same type of intermediates should be involved.[36] Catalases, which like peroxidases catalyze hydrogen peroxide activation, are different from peroxidases in the sense that the proximal amino acid binding directly to the heme iron is tyrosine, which cannot be hydrogen bonded to a carboxylate as the proximal histidine of peroxidases is. In the present study the histidine was modeled by a neutral imidazole, while for catalases the proximal heme ligand has to be modeled by a negatively charged phenolate. The effects of different proximal amino acids are currently under investigation and will be discussed in a future paper.

JA991997C

(36) Blomberg, M. R. A.; Siegbahn, P. E. M.; Babcock, G. T.; Wikström, M. Submitted for publication.